International Journal of Mosquito Research

ISSN: **2348-5906**
CODEN: **IJMRK2**
IJMR 2018; 5(5): 37-43

Received: 25-07-2018
Accepted: 26-08-2018

**Danilo A Gualberto**
Department of Biology, College of Arts and Sciences, Xavier University, Cagayan de Oro City, Philippines

**Cesar G Demayo**
Department of Biological Sciences, College of Science and Mathematics, MSU-Iligan Institute of Technology, Iligan City, Philippines

**Correspondence**
**Cesar G Demayo**
Department of Biological Sciences, College of Science and Mathematics, MSU-Iligan Institute of Technology, Iligan City, Philippines

# Describing wing shape variations within, between and among populations of *Aedes albopictus* Skuse using relative warp analysis

**Danilo A Gualberto and Cesar G Demayo**

**Abstract**
Population variations in one of the Dengue vector mosquitoes, *Aedes albopictus* (Skuse) was examined using landmark-based Geometric Morphometric analysis of the shapes of their wings. Wing shape variations within, between and among sexes of three populations of *Ae Albopictus* were compared. MANOVA of Relative warp scores of the landmark coordinates as variables show the Wilk's lambda has very low values ($\lambda$~0.1733 – 0.2553), indicating that wing shapes were distinguishable between the three mosquito populations. MANOVA pairwise comparisons of wing shape scores showed significant differences between the population structures of *Ae. Albopictus* based on the wing shapes of individual mosquitoes. Relative warp analysis of wing scores yielded between 3 to 7 significant principal components that explained the nature of variations in the mosquito wings of the three populations. Results of this study have clearly shown that the mosquitos vary and the variations can be attributed to the variations among individuals within each of the populations.

**Keywords:** *Aedes,* MANOVA, geometric morphometrics, shape, relative warps

## 1. Introduction
Infraspecific variations has been observed in two dengue vectors *Aedes aegypti* [1, 2, 3, 4] and *Ae. Albopictus* populations [5, 6. 7, 8]. Global migration route and population disruptions due to repeated vector control measures, are argued to induce genetic [1-4] and subsequent morphological variations [1]. It is argued that *Ae. Albopictus'* migrations to different regions may have induced adaptive changes to different environments and these may have been reflected in wing shape differentiations. A study using canonical variate analysis of wing shapes of *Ae. Albopictus* show wing variations for just a period of 4 years of study [6]. To be able to assess variations in microgeographic scale in *Ae. Albopictus*, populations were compared based on the shapes of their wings. Since the wings are considered the most excellent structures for studying morphological variations because wing vein intersections provide well-defined landmarks suitable for morphometric studies, it is used to compare population structures and variations. The metric properties of the wings provide very precise information for population variation studies. Geometric morphometric (GM) properties of insect wings, for example, has been cited to provide precise quantitative information for the identification of species complexes as well as within-species variations [9-13], for discrimination of sibling species of Neurothemis dragonflies [12], as well as for showing intraspecific variations of rice black bugs [13]. We use this methodology in the assessment of morphometric variability in wing shapes of the three populations of *Ae. Albopictus* which are found in the vicinity of Cagayan de Oro City, areas which are reported by the Department of Health (DOH) to have cases of dengue. These populations were from rural villages to urban dwellings in the city. The determination of population variations in *Ae. Albopictus* will be evaluated using landmark-based geometric morphometrics specially the application of relative warp analysis. The research hypothesis of this study was that *Ae. Albopictus* may each have distinct morphological differences that can be manifested in wing shapes.

## 2. Materials and Methods

### 2.1 Sampling sites

Specimens of *Ae. Albopictus* were collected from 3 ecologically and socioeconomically distinct areas in the city namely: coastal, poblacion, and rural (Fig. 1) based on basic distinctions of these areas that are arbitrarily described as follows:

**2.1.1 Coastal areas:** These comprises of a narrow 25 km stretch of 11 political territories, called villages, fronting the Macajalar bay of Cagayan de Oro City. These areas were often subject to dessicating salt-bearing breeze that comes from the sea and temperatures that fluctuate daily due to daily rhythms of land-bound and sea-bound winds in coastal regions. The microclimates found in these areas may pose developmental effects to the *Ae.* Mosquitoes. Factories, storage sites (bodegas), small stores and human habitations mostly belonging to families below the poverty line were abundant and squatter areas commonly line some segments of the unclaimed coastal areas.

**2.1.2 *Poblacion*:** These were flat inland territories located at the lowland areas of Cagayan de oro that was no more than 10 meters above the sea-level. This area, about 4214 $km^2$, were divided into 40 small villages, and were heavily congested with long-established residences (in the 1960s or before) and stores, malls and markets. Temperatures and humidity were less changeable in these areas except during long periods of dry spells or heavy rains. Most of the residents belong to the middle socioeconomic class with well-maintained water pipe systems

**2.1.3 Rural areas:** These areas were located in the upland areas of Cagayan de Oro City which were characterized by mountains, hills, plateaus and gorges. The areas are covered with a lot of vegetation and forests with paved and unpaved roads. A good number of high-income households were found among low-income households in the rural areas. The current developments in these areas included production plants and human housing complexes or subdivisions.

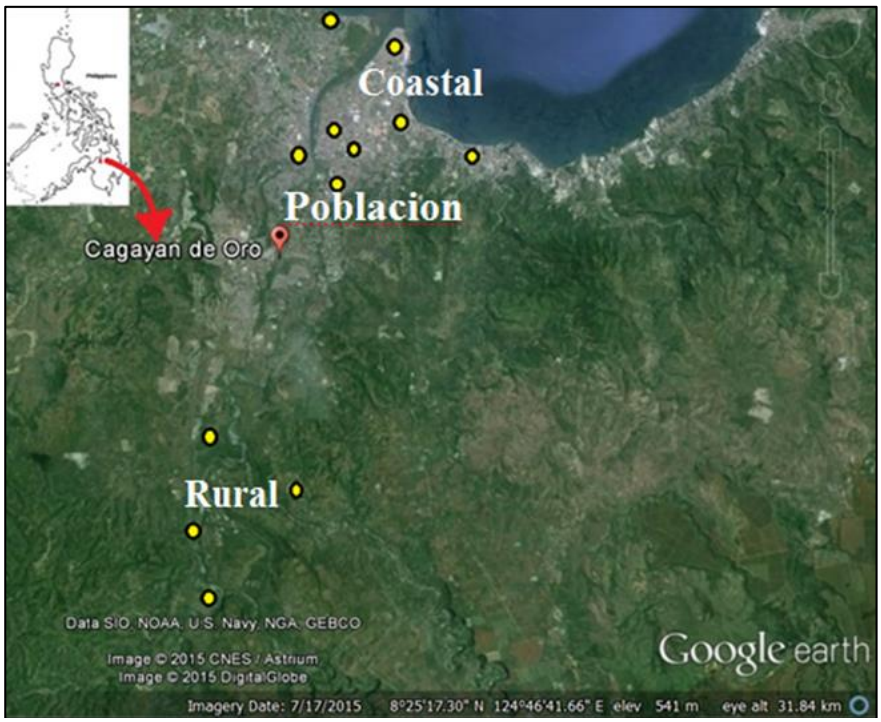


**Fig 1:** Google-earth Satellite image of Cagayan de Oro City and the locations (in yellow dots) of sampling sites in coastal, poblacion and rural areas of the City.

### 2.2 Collection of mosquito samples

Larvae and pupae of *Ae. Albopictus* were collected mainly from stagnant water inside abandoned or unused tires that were commonly found in vulcanizing shops in the selected villages or abandoned areas in the three sampling areas in Cagayan de Oro City. These were done by suctioning them using a kitchen baster and were immediately transferred into mineral water bottles with the sediments. The bottles were capped and secured in softdrink cases to keep them stable during transport from the sampling sites to the laboratory.

### 2.3 Rearing of mosquito larvae to adulthood

In the laboratory, the sample bottles were converted into rearing bottles by removing the caps of the sample bottles and then replacing them with 7.25 cm x 4 cm pvc pipes that were topped with textile netting material. These pvc pipes with net were secured to the neck of the rearing bottles by putting pieces of masking tape between the pipe and bottle so that the pvc pipes served as "chimney" that kept air flowing into the rearing bottles as well as prevent emerge adults from flying out. The rearing of *Aedes* from pupae to adult usually took about a day or two before the pupae hatched into adults.

### 2.4 Preparation of adult hatchlings

As adults emerged, the adult mosquitoes were released into 30 cm x 30 cm cages and asphyxiated in killing bottles laced

with ethyl acetate. The dead mosquito adults from each rearing bottles were then transferred into delicups with appropriate labels for systematic recording. The asphyxiated adult mosquitoes were kept for 2-3 days in delicups before their wings were clipped to avoid tearing. Freshly killed adult specimens usually have wings that easily tear when these are removed just a few hours after asphyxiation.

In the laboratory, the dead adult hatchlings were transferred into a watch glass and observed under the binocular stereomicroscope. The adult mosquitoes are then sorted according to species and sex. Scutal patterns of white or silvery scales and other scale patterns were used in the identification of *Ae. Albopictus* species. Antennal types were used for sorting *Aedes* adult mosquitoes into female and male sexes. Female and male adult *Ae. Albopictus* were segregated from non-*Aedes* adults. With ocular guidance under the binocular stereomicroscope, the left and right wings were removed by gently nudging the wings with dissecting needle from the mosquito body and were then placed on a microscope slide. Both left and right wings per adult were mounted side by side on clean microscope slides. About 5-15 pairs of left and right wings per species were mounted and secured with another glass slide over it. The glass slides with mounted wings were glued with small amounts of cyanoacrylate adhesives at the sides. A total of 30 wings each from female and male adults from the 3 selected locations were mounted and prepared for the entire study.

Images of individual wings were then captured as jpeg images under 4x objective lens with Leica DM2700 Microscope coupled to a digitizing software LAS EZ 3.0. The jpeg images of left and right wings from were then saved in separate folders in the computer for geometric morphometric analyses.

### 2.5 Acquisition of data for Landmark-based Geometric Morphometrics

For each jpeg images of wings, 20 landmarks in the wings were identified [11] and digitized using the application of tpsDig software [14] (see Fig. 2, Table 1). The 30 pairs of left and right wings were digitized thrice to yield a total of 90 jpeg images of left and right wings to be landmarked separately. The raw coordinates of the 20 landmarks were then subjected to Procrustes superimposition and thin-plate spline analyses to generate "relative warp" scores [15]. Affine variation (the "uniform component"), were computed separately, and added to the partial warp scores to constitute the final set of shape variables, i.e. variables describing the displacement of each landmark relative to the consensus wing.

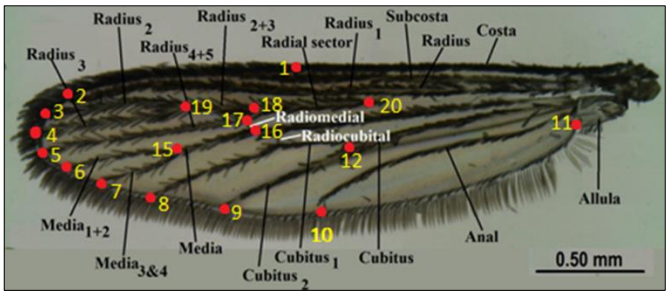


**Fig 2 (a):** The 20 landmarks created from TpsDig2 software from a labelled generalized mosquito wing, image courtesy of WRBU Mosquito Identification software, WRBU.

**Table 1:** The designated number and location of landmarks used in the study.

| No. | Location of landmark | No. | Location of landmark |
|---|---|---|---|
| 1 | Junction of costa and subcostal | 11 | Axillary incision (distal notch of the alula) |
| 2 | Distal end of the first branch of radius | 12 | Posterior point of the mediocubital crossvein |
| 3 | Distal end of the second branch of radius | 13 | Anterior point of the mediocubital crossvein |
| 4 | Distal end of the third branch of radius | 14 | Forkpoint between M (median vein) and $M_{3+4}$ |
| 5 | Distal end of radius $_{4+5}$ | 15 | Fork point of the $M_1$and $M_2$ |
| 6 | Distal end of M $_{1+2}$ branch | 16 | Posterior point of the radiomedial crossvein |
| 7 | Distal end of M $_{3+4}$ | 17 | Anterior point of the radiomedial crossvein |
| 8 | Distal end of the first branch of the cubitus (Cu1) | 18 | Forkpoint between $R_{2+3}$ and $R_{4+5}$ |
| 9 | Distal end of the second branch of the cubitus (Cu2) | 19 | Forkpoint of $R_2$ and $R_3$ |
| 10 | Distal end of the anal vein | 20 | Forkpoint of $R_1$ and Rs (radius sector) |

### 2.6 Analysis of Data

#### 2.6.1 Landmark-based geometric morphometric Analysis

Initially, the x and y coordinates of the 20 landmark points taken from all left and right wings of both sexes were used to generate thin-plate spline (tps) files and links files using TpsDig software [14]. Separate tps files of the coastal, poblacion and rural wing samples were then appended and pooled using tpsUtil software [16]. These pooled tps files were then run in tpsRelw software [15] separately to generate the relative warp scores for the left and right wings of each sexThin-plate spline images were saved from tps Relw visualization plots that were also generated from pooled tps files.

#### 2.6.2 Relative warp analysis

In generating the relative warp scores in tpsRelw, the landmark configurations were scaled, translated, and rotated against consensus configuration by General Least Squares – Procrustes superimposition method in 2D. The differences in thin-plate spline ordination plot were then used to describe the scaled wing shape differences between sexes *Ae. Albopictus*. Only relative warp scores above 5% were described and compared.

#### 2.6.3 Multivariate Analysis of Variance

Pooled relative warp (RW) scores that were generated in tpsRelw from pooled tps files of the three populations were run in Multivariate Analysis of Variance (MANOVA) using Paleontological Statistics, PAST version 2.17c [17]. But prior to MANOVA, the scores were first tested for normality with Shapiro-Wilk statistics that have *p* values that are less than the alpha level (0.05) to test whether the null hypothesis must be

rejected and that evidence indicates that data tested are not a normally distributed population. The wing shape RW scores were then subjected to MANOVA to test whether or not the means for two or more groups are sampled from the same sampling distribution based on two common multivariate test criteria: 1) Wilks' lambda and 2) Pillai's trace. A small Wilk's lambda (close to 0) indicates that the groups are well separated, but a large Wilk's lambda (close to 1) points to the fact the groups of variables are poorly distinguishable from one another [13]. Pillai trace determines the independence between groups of variables. The greater the value of Pillai's trace, the more the given effect contributes to the model. A posthoc test with Hotelling's pairwise comparison were also generated in MANOVA to determine which variable sets were significantly different from each other.

## 3. Results and Discussion

The CVA analysis showed very low Wilk's lambda ($\lambda$~0.1733–0.2553). The Wilk's lambda for both sexes based on the left and right wings yielded very low values, which indicated that the wing shape scores in the three population's coastal, poblacion and rural samples of female *Ae. Albopictus* were very distinctive in their distributions (Table 2). Pillai's trace values that ranges between 0.959-1.138 also implied that there were independence of the relative warp scores in female and male *Ae. Albopictus* from the three populations and are suggestive of wing shapes that have varying developmental trajectories. The variations are graphically shown in a scatter plot generated showing the distribution of individuals within and between sexes (Fig. 3). Relative warp analysis in female *Ae. Albopictus* wings explained a total of 77.58% of the observed variations in the left and 76.49% in the right wing shapes. For the male, a total of 77.42% describes the left and 76.69% for the variations in the right wing. A total of 7 relative warps were identified for female *Ae. Albopictus* left wings that comprised 77.58% of all variations.in wing shapes. Seven (7) significant relative warps, comprising 77.58% of all variations in the right wing shapes were also identified in the right wings. These nature of these variations are described in Table 3 and 4. MANOVA showed significant differences in wing shapes between populations within sexes (Table 5).

**Table 2:** Wilk's lambda and Pillai trace for left and right wing shape scores in female and male populations of *Ae. Albopictus*

| Wing shapes | Wilk's λ | Pillai's trace |
|---|---|---|
| ♀ *A. Albopictus* left | 0.2553 | 0.959 |
| ♀ *Ae. Albopictus* right | 0.2314 | 1.024 |
| ♂ *Ae. Albopictus* left | 0.1892 | 1.119 |
| ♂ *Ae. Albopictus* right | 0.1733 | 1.138 |

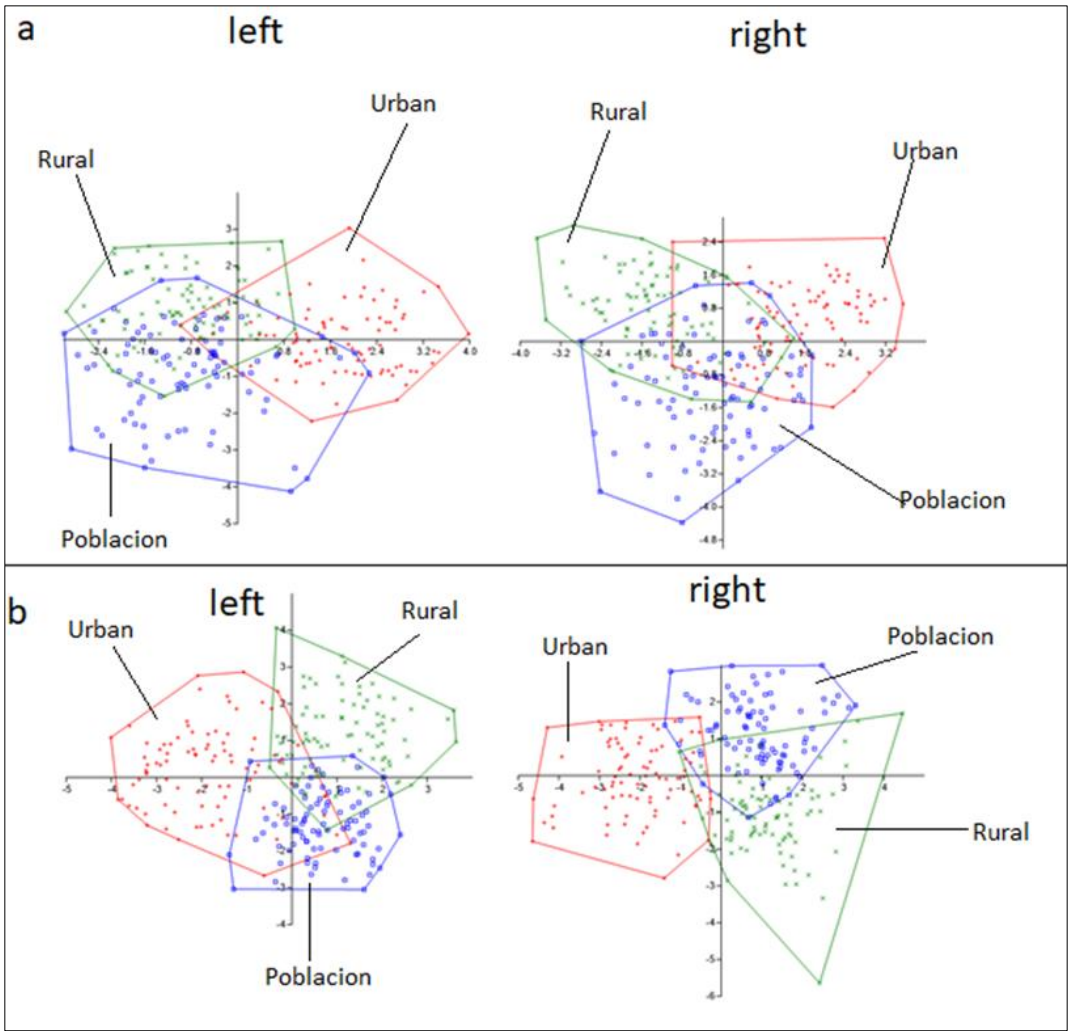


**Fig 3:** MANOVA CVA scatter plot of left and right wings of female (A) and male (b) *Ae. Albopictus*

**Table 3:** Descriptions and variations in the landmarked-based points of left and right female *Ae. Albopictus* wing shape.

| Relative warp | Left wing | Relative warp | Right wing |
|---|---|---|---|
| RW 1 (22.59%) | Landmark 10 and 12 are the most displaced vector units. In the RW visualization plot, landmark 10, 11 and 12 vector are displaced away from each other that cause expansion at the tailing edge of the wing. | RW 1 (21.3%) | Displacements of vector units at landmarks 10, 11, and 12 located near and at the wing base have expansions of the basal regions of the wing, while compressions are occurring at the distal edges of the wing. |
| RW 2 (14.84%) | The vector unit that is most displaced are landmarks 5, 6, and 7, as well as landmark 11 at the alular notch of the wing base. Landmark 11 displaced towards the body, causing extension of the entire wing starting from the base. Very slight displacements are detected at the apically-located landmarks 5, 6 and 7 causing expansion in the deformation grids. | RW 2 (13.84%) | The vector unit that is most displaced are landmarks 13, 14, 16, and 18 at the radio-cubital and medio-cubital veins. |
| RW 3 (10.89%) | The variation is mainly due to landmarks 1, 12 and 20 that are in opposite directions causing expansion. | RW 3 (11.77%) | Variation is mainly due to landmarks 12, 18 and 20 that are separating, yielding expansion at the middle region of the wing. |
| RW 4 (10.18%) | This variation is due to opposite displacements of landmarks 15, 16, 17, and 18 resulting to expansion/dilation near the medio-cubitus regions. | RW 4 (9.85%) | Slight separation of landmarks 16, 17, and 18 resulted to expansion/dilation near the medio-cubitus vein and the extension of the lower distal edge of the wing. |
| RW 5 (7.36%) | Landmarks 1, 9 and 20 are the most displaced vector units causing small expansion at the leading edge and tailing edge of the wing. | RW 5 (8.1%) | Landmarks 1 and 20 are the most displaced vector units causing small expansion at the leading edge of the wing shape. Small displacement of landmark 8 also accounts for a distal expansion in the distal region of the wing shape. |
| RW 6 (6.57%) | The displacement in this variant is due to diverging displacement at landmark 1 and 18 as well as landmark 8 that is directed away from the wing base, thereby causing expansion of the wing. | RW 6 (6.19%) | The most significant displacement in this variant occurs at landmark 1 that is directed to the wing base, thereby causing expansion of the wing. |
| RW 7 (5.15 %.) | The diverging displacements of landmark 1 towards the wing base and the distal displacements of landmarks 8, 9 and 15 resulted to an expansion at the distal region of the wing shape. | RW 7 (5. 36 %.) | The distally-directed displacement at landmark 6 results to an expansion at the distal region of the wing shape. |

**Table 4:** Descriptions and variations in the landmarked-based points of pooled left and right male *Ae. Albopictus* wing shape.

| Relative warp | Left wing | Relative warp | Right wing |
|---|---|---|---|
| RW 1 (23.2%) | Displacements of vector units at landmarks 9 and10 located at the tailing edge of the wing yield expansions of anal region of the wing, while compressions are occurring at the leading edges of the wing. | RW 1 (24.16%) | Landmark 9 is the most displaced vector unit in this relative warp, yielding expansion in the tail end of the wing. |
| RW 2 (19.72%) | Extensions at landmarks 2, 3, 4 and 5 at the radius 1, 2, 3, & 4+5 and landmark 11 yield expansion at the distal and basal ends of the wing. Compressions at the middle of the wings appear to oppose these expansions. | RW 2 (14.37%) | The vector unit that is most displaced in RW 2 is landmark 2-7 at the distal edge of the wing and landmark 11 at the alular notch of the wing base. Expansions therefore has occurred at the two ends of the wing, while compression occurs at the middle of the wing. |
| RW 3 (14.37%) | Variation is mainly due to landmarks 12 and 20 that are separating, yielding expansion at the middle region of the wing. | RW 3 (12.71% | The greatest expansion occurs at the landmark 8 and 9 at the tailing edge of the wing and at landmark 11 at the wing base. |
| RW 4 (7.91%) | Variations in left male *Ae. Albopictus.* Slight extensions of landmarks 3, 4, 5, 6, and 7 resulted to dilation of the distal edge of the wing. There is also compression at the landmarks 14, 15, 16, and 18. | RW 4 (10.08%) | This variation is due to displacements of landmarks 2, 8, 9, 12 and 20. Their relative shearing vectors resulted to expansion/dilation near the medio-cubitus vein and the extension of the lower distal edge of the wing. |
| RW 5 (6.97%) | Landmarks 12 and 20 are the most displaced vector units causing small expansion at the leading edge of the wing shape. Small displacement of landmark 4 also accounts for a distal expansion in the distal region of the wing shape. | RW 5 (6.89%) | Landmarks 9 and 10 are the most displaced causing small expansion at the tailing edge of the wing. |
| RW 6 (5.25%) | The most significant displacement in this variant occurs at landmark 1 that is directed to the wing base, thereby causing expansion of the wing. | RW 6 (5.66%) | The largest displacement in this variant occurs at landmark 1 that is directed to the wing base, thereby causing expansion of the wing. |

**Table 5:** MANOVA pairwise comparisons in the left and right wing shapes of *Ae. Albopictus* between locations in Cagayan de Oro City.

| | | Left Wing | | Right Wing | |
|---|---|---|---|---|---|
| | | **Poblacion** | **Rural** | **Poblacion** | **Rural** |
| Female | Coastal | 2.72E-19 | 3.01E-19 | 2.58E-15 | 1.95E-21 |
| | Poblacion | | 2.87E-07 | | 8.41E-13 |
| Male | Coastal | 4.92E-21 | 2.51E-23 | 4.92E-21 | 2.51E-23 |
| | Poblacion | | 1.12E-14 | | 1.12E-14 |

## 4. Discussion

In a seminal paper by McDonnell and Pickett [18] it was suggested that "urbanization" is not just to be taken as an anthropological development, but should also a complex phenomenon for environmental alterations that usher population changes that impact both man and other living organisms, especially disease vectors like the mosquitoes. Preliminary collections and observations in previous unpublished studies have shown that 2 mosquito species *Ae. Aegypti* and *Ae. Albopictus* are the most common and abundant diurnal mosquitoes in the urbanized environments of Cagayan de Oro City. During a one-year GIS-aided ovitrap surveillance of the immature *Ae.* Mosquitoes, larval rearing of the same mosquitoes have shown that various forms of these *Aedes* mosquitoes exist [19]. Since the wings are used in migration and eventual adaptation in the communities where they settled, the variations could be reflected in their wing geometry and thus variability in different populations of the mosquito would be manifested as shown in this study. The results in this study are also in conformity of the nature of wing shape variations in several species of mosquitoes earlier investigated using GM methods. GM methods not only has been successfully used for distinguishing different laboratory-reared *Ae. aegypti* lines over many generations [11], for species determination [6, 7], interspecific overlapping between *Ae. Aegypti* and *Ae. Albopictus* [5], variations in wing shapes between *Aedes* namely, *Ae. aegypti*, *Ae. Albopictus* and *Ae. Pseudotaeniatus* [8, 20], and wing shape changes as suggestive of genetic drift [11].

## 5. Conclusion

Since the wings are used in migration and eventual adaptation in the communities where they settled, the variations could be reflected in their wing geometry and thus variability in different populations of the mosquito would be manifested as shown in this stud

## 6. Acknowledgement

The senior author would like to acknowledge the Commission on Higher Education for the scholarship grant and the Premier Institute of Science and Mathematics (PRISM) of the MSU-Iligan Institute of Technology for the grant.

## 7. References

1. Brown JE, V Obas, V Morley, JR Powell. Phylogeography and Spatio-Temporal Genetic Variation of *Aedes aegypti* (Diptera: Culicidae) Populations in Florida Keys. J. Med. Entomol. 2013; 50(2):294-299.
2. Jupp PG, Kemp A, Frangos C. The potential for dengue in South Africa: Morphology and taxonomic status of *Aedes aegypti* populations. Mosq. Syst. 1991; 23(3):182-190.
3. Katyal R, Gill KS, Kumar K. Seasonal Variations of *Aedes aegypti* population in New Delhi, India. Dengue Bull. 1996; 20:78-81.
4. McClelland GAH. A World-wide Survey of Variation in Scale Pattern of the Abdominal Tergum of *Aedes aegypti* (L.) (Diptera: Culicidae) Trans. Royal Entomol. Soc. London. 26(2):239-259.
5. Henry A, Thongsripong P, Fonseca-Gonzalez I, Jaramillo-Ocampo N, Dujardin JP. Wing Shape of Dengue Vectors from around the World. Infec. Gen. Evol. 2010; 10:207-214.
6. Vidal PO, Suesdek L. Comparison of Wing Geometry Data and Genetic Data for Assessing the Population Structure of *Aedes aegypti*. Inf., Gen. Evo. 2012; 12:591-596.
7. Vidal PO, Carvalho E, Suesdek L. Temporal variation of wing geometry in *Aedes albopictus.* Mem. Inst. Oswaldo Cruz, 2012, 107(8).
8. Mondal1 R, Pemola Devi N, Jauhari RK. Landmark-based geometric morphometric analysis of wing shape among certain species of *Aedes* mosquitoes in District Dehradun (Uttarakhand), India. J Vector Borne Dis. 2015; 52:122-128.
9. Calle Da L, Quinones ML, Erazo HF, Jaramillo ON. Morphometric discrimination of females of five species of *Anopheles* of the subgenus Nyssorhynchus from Southern and Northwest Colombia. Mem Inst Oswaldo Cruz. 2002; 97:1191-5.
10. Villegas J, Feliciangeli MD, Dujardin JP. Wing shape divergence between *Rhodnius prolixus* from Cojedes (Venezuela) and *Rhodnius robustus* from Mérida (Venezuela) Infection, Genetics and Evolution 2002; 2:121–128.
11. Jirakanjanakit N, Leemingsawat S, JP Dujardin. The Geometry of the Wing of *Aedes* (Stegomyia) *aegypti* in isofemale lines through Sucessive Generations. Infect. Gen. Evol. 2008; 8:414-421.
12. Demayo CG, Harun SA, Torres MAJ. Procrustes analysis of wing shape divergence among sibling species of *neurothemis* dragonflies. Aust. J. Basic Applied Sci., 2011; 5:748-759.
13. Torres MAJ, Figueras GS, LuceÑo AJM, Patiluna MLE, Manting MME, Rampola RB, *et al*. Describing phenotypic diversity in an outbreak population of Rice Black Bugs from Balangao, Diplahan, Zamboanga Sibugay, Philippines using principal component analysis and K-means clustering of morphological attributes. AES Bioflux. 2013; 5(1):15-22.
14. Rohlf FJ. Version 1.40. New York: Department of Ecology and Evolution, State University of New York at Stony Brooks. 2004.
15. Rohlf FJ. TpsRelw for Windows v. 1. 17, Thin-Plate Spline Relative Warps Analysis. Department of Ecology and Evolution, State University of New York, Stony Brook, NY 11794-5245. (Available by ftp from life. Bio. SUNYSB. edu/ Morphmet), 1998.
16. Rohlf FJ. Version 1.28. New York: Department of Ecology and Evolution, State University of New York at Stony Brook, 2004.
17. Hammer OH, Harper DAT, Ryan PD. Paleontological Statistics Software Package for Education and Data

Analysis. Paleontologia Electronica, 2001; 4(1):9. http;//paleoelectronica.org/2001_1/past/issue1.01.htm
18. McDonnell MJ, Pickett STA. Ecosystem Structure and Function along Urban-Rural Gradients: An Unexploited Opportunity for Ecology. Ecology. 1990; 71(4):1232-1237.
19. Gualberto D, Sabines MD, Demayo CG. Use of modified autocidal ovitraps predetermined by GPS and GIS for surveilalance of dengue mosquito vectors in Cagayan de Oro City, Philippine. Advances in Environmental Biology. 2015; 9(25):1-9.
20. Sendaydiego J, Torres MA, Demayo CG. Describing Wing Geometry of *Aedes aegypti* Using Landmark-Based Geometric Morphometrics. Int. J Biosci, Biochem. Bioinfo. 2013; (4):379-38.